JVI Journals.ASM.org

Insight into the Mechanism of Inhibition of Adeno-Associated Virus by the Mre11/Rad50/Nbs1 Complex

Thomas B. Lentz,[a] R. Jude Samulski[a,b]

Gene Therapy Center[a] and Department of Pharmacology,[b] University of North Carolina, Chapel Hill, North Carolina, USA

ABSTRACT

Adeno-associated virus (AAV) is a dependent virus of the family *Parvoviridae*. The gene expression and replication of AAV and derived recombinant AAV (rAAV) vectors are severely limited (>10-fold) by the cellular DNA damage-sensing complex made up of Mre11, Rad50, and Nbs1 (MRN). The AAV genome does not encode the means to circumvent this block to productive infection but relies on coinfecting helper virus to do so. Using adenovirus helper proteins E1B55k and E4orf6, which enhance the transduction of AAV via degradation of MRN, we investigated the mechanism through which this DNA damage complex inhibits gene expression from rAAV. We tested the substrate specificity of inhibition and the contribution of different functions of the MRN complex. Our results demonstrate that both single- and double-stranded rAAV vectors are inhibited by MRN, which is in contrast to the predominant model that inhibition is the result of a block to second-strand synthesis. Exploring the contribution of known functions of MRN, we found that inhibition of rAAV does not require downstream DNA damage response factors, including signaling kinases ATM and ATR. The nuclease domain of Mre11 appears to play only a minor role in inhibition, while the DNA binding domain makes a greater contribution. Additionally, mutation of the inverted terminal repeat of the rAAV genome, which has been proposed to be the signal for interaction with MRN, is tolerated by the mechanism of inhibition. These results articulate a model of inhibition of gene expression in which physical interaction is more important than enzymatic activity and several key downstream damage repair factors are dispensable.

IMPORTANCE

Many viruses modulate the host DNA damage response (DDR) in order to create a cellular environment permissive for infection. The MRN complex is a primary sensor of damage in the cell but also responds to invading viral genomes, often posing a block to infection. AAV is greatly inhibited by MRN and dependent on coinfecting helper virus, such as adenovirus, to remove this factor. Currently, the mechanism through which MRN inhibits AAV and other viruses is poorly understood. Our results reform the predominant model that inhibition of rAAV by MRN is due to limiting second-strand DNA synthesis. Instead, a novel mechanism of inhibition of gene expression independent of a block in rAAV DNA synthesis or downstream damage factors is indicated. These findings have clear implications for understanding this restriction to transduction of AAV and rAAV vectors, which have high therapeutic relevance and likely translate to other viruses that must navigate the DDR.

Adeno-associated virus (AAV) is a member of the genus *Dependovirus* within the family *Parvoviridae*. The virion is small (diameter, ~20 nm) and consists of a protein nucleocapsid containing a single-stranded DNA (ssDNA) genome of ~4.7 kb. The genome carries inverted terminal repeat (ITR) sequences at both ends, which self-anneal to form a T-shaped secondary structure (1, 2). Formation of this structure provides the 3′ OH for second-strand DNA synthesis, as well as the signal for genome packaging. Flanking ITRs are the only feature required in *cis* for replication and production of the virus. This property is exploited in recombinant AAV (rAAV) vectors, in which the coding region of the genome is replaced with a transgene expression cassette (3). The AAV genome carries two genes encoding replication (Rep) and capsid (Cap) proteins (4). Both are required for replication and packaging of AAV and are provided in *trans* for production of rAAV vectors. However, these proteins are not sufficient. Wild-type (wt) AAV and rAAV are dependent upon helper virus and host cell proteins for creation of a permissive cellular environment and DNA synthesis machinery, respectively (5, 6).

Establishment of a permissive cellular environment for expression and replication of AAV requires mediation of the cellular DNA damage response (DDR). DDR signaling and repair pathways normally function in maintenance of the cellular genome. However, these pathways can be activated during viral infection, adopting auxiliary, often antagonistic roles when confronted with foreign genetic material (7, 8). The AAV genome does not encode a mechanism to mediate the DDR but requires helper virus to accomplish this. In the absence of helper virus, wt AAV and rAAV provoke only minor damage signaling in the form of phosphorylation of γ-H2AX (9, 10). During such infections, gene expression is muted and the virus may circularize or integrate into the host genome, as is the case with wt AAV in the presence of Rep proteins, resulting in latency (11, 12). Coinfection with AAV and the adenovirus (Ad) helper (i.e., productive infection) produces ro-

Received 9 July 2014 **Accepted** 3 October 2014

Accepted manuscript posted online 15 October 2014

Citation Lentz TB, Samulski RJ. 2015. Insight into the mechanism of inhibition of adeno-associated virus by the Mre11/Rad50/Nbs1 complex. J Virol 89:181–194. doi:10.1128/JVI.01990-14.

Editor: M. J. Imperiale

Address correspondence to R. Jude Samulski, rjs@med.unc.edu.

doi:10.1128/JVI.01990-14

bust DDR signaling, involving activation of the kinases DNA-dependent protein kinase (DNA-PK) and ATM and downstream targets, including Chk1 and Chk2 (10, 13). Activation of these pathways is provoked by AAV genome replication but appears to be regulated in a manner that benefits the virus. The activity of DNA-PK has been demonstrated to enhance AAV replication, possibly via a role in processing of the ITRs (14, 15). In contrast, the complex made up of Mre11, Rad50, and Nbs1 (MRN) restricts AAV replication and is downregulated by Ad proteins during coinfection (16).

MRN plays a critical role in the permissiveness of a cell to transduction by AAV and other viral and nonviral pathogens (7, 17). This complex normally functions as a sensor of DNA damage in the cell and participates in the homologous recombination (HR) and nonhomologous end joining (NHEJ) pathways of repair (18–21). MRN accumulates at foci on cellular DNA within minutes after insult (22, 23). It then initiates damage signaling involving activation of ATM and ATR kinases (24–26). During infection with AAV, MRN is recruited to the viral genome shortly after introduction and dramatically limits the activity of the virus (27). Coprecipitation from the cell lysate and interaction of purified Mre11 and Nbs1 proteins with an oligonucleotide representing the viral ITR *in vitro* suggest a direct interaction with the viral genome, possibly via the terminal hairpin structures (16, 27). Knockdown of proteins of the MRN complex with short hairpin RNA (Rad50) or small interfering RNA (Nbs1) leads to enhancement of virus, and fibroblasts deficient for Mre11 are highly permissible to transduction (16, 27). Additionally, the permissiveness of muscle cells to rAAV *in vivo* correlates with the loss of MRN during differentiation (28). During productive infection, coinfecting helper viruses remove this block to infection. Herpes simplex virus (HSV) utilizes MRN during replication and recruits this complex to its genome (29–31). This may have the effect of sequestering MRN, thus relieving inhibition and contributing to the enhancement of AAV observed with HSV. In contrast, Ad, like AAV, is inhibited by MRN and expresses mechanisms to remove this barrier. Early proteins E1B55k and E4orf6 form an E3-like ubiquitin ligase complex and target MRN for degradation (32). In a redundant mechanism, early protein E4orf3 relocalizes the complex to the cytoplasm, away from the viral genome (33, 34). The dependence of AAV on helper viruses to remove MRN for productive infection indicates the severity of the inhibitory effect. However, the mechanism of inhibition of AAV by MRN is not well understood.

Here, we investigate the mechanism of MRN inhibition of gene expression from rAAV genomes, in which the viral promoters and genes have been replaced with a reporter gene expression cassette. Previous studies have found that the degradation of MRN by E1B55k/E4orf6 leads to increased second-strand DNA synthesis for AAV (35, 36). This result has been interpreted to suggest that MRN blocks completion of the genome, which has been proposed to be the mechanism of inhibition. Using Ad proteins E1B55k and E4orf6 as a tool to track inhibition by MRN, we tested this model and found that double-stranded rAAV vectors, which do not require second-strand DNA synthesis for gene expression, are enhanced in a manner similar to that for single-stranded vectors. Probing further into the nature of this mechanism, we investigated the contribution of downstream DNA damage signaling and repair factors and the specific activities of Mre11. Analysis of cell lines deficient for DDR factors downstream of MRN indicates that key signaling kinases ATM and ATR, as well as factors important for the HR and NHEJ repair pathways, are not required for inhibition. Additionally, the contribution of the nuclease activity of Mre11 appears to be minor. Instead, our findings implicate a role for the DNA binding domain of Mre11. In an effort to understand the importance of the ITR to this interaction, mutation of this feature was performed and indicates that sequence and structure may already be optimized to limit the effect of MRN. Together, these results suggest that a direct interaction may be more important to the mechanism of inhibition of rAAV than the enzymatic or signaling activities of MRN.

MATERIALS AND METHODS

Plasmids. Plasmids pXR2 (AAV serotype 2 [AAV2] Rep/Cap donor) and pXX6-80 (adenovirus protein donor) have been described previously (37, 38). Plasmids pTR2-CMV-eGFP-Neo, pTR2-CMV-Luc, and pTR2-CBA-Luc harbor a single-stranded AAV genome flanked by serotype 2 ITRs and contain either the human cytomegalovirus (CMV) major immediate early or chicken β-actin (CBA) promoter driving the expression of either the enhanced green fluorescent protein (eGFP) or luciferase transgene (39–41). The Ad serotype 5 (Ad5) E1B55k gene was amplified from the genomic DNA of HEK293 cells, which carry the E1 region of Ad5, with primers Ad5 SalI/AgeI 2019-2042+ (5′-GACGTCGACCGGTATGGAG CGAAGAAACCCATCTGAG-3′) and Ad5 NotI 3479-3509 (5′-CCGCG GCCGCTCAATCTGTATCTTCATCGCTAGAGCCAAAC-3′). The PCR product was ligated into the plasmid pTR2-CMV-eGFP-Neo using the AgeI and NotI restriction sites to produce pTR2-CMV-E1B55k-Neo. Plasmid pdsEMBLgfp4 harbors a self-complementary AAV (scAAV) vector genome flanked by one wt and one defective serotype 2 ITR and contains the CMV promoter driving the expression of eGFP (a kind gift from X. Xiao). Plasmid pdsEMBL-CMV-E4orf6 (pMH210) was constructed by BamHI excision of the adenovirus E4orf6-coding sequence from pCMV-E4orf6 (a kind gift from P. Hearing), treatment with the Klenow fragment to blunt the ends, and ligation into blunt-ended AgeI and NotI sites of pdsEMBLgfp4 (42). Plasmids pDD2-eGFP, pDD5-eGFP, pDD5+2SNS-eGFP, and pDD2+5NS-eGFP have been described previously and consist of a single wild-type or mutant ITR in DD form inserted along with a CMV-eGFP expression cassette into the pUC18 backbone (43, 44). Plasmid pTRSn-CMV-eGFP was generated by substitution of a CMV-eGFP expression cassette, flanked by PstI and PciI restriction sites, for the majority of the genome in the snake AAV construct pSAAV (a kind gift from Peter Tijssen) via compatible PstI and NcoI restriction sites (45). A donor plasmid for expression of the snake AAV Rep protein was generated in order to produce the TRSn-CMV-eGFP vector. The snake AAV Rep gene was amplified from pSAAV and fused with the AAV serotype 2 Cap gene (with the AAV2 Cap replacing the snake Cap sequence) by overlap extension PCR. This fragment was then substituted for the wt AAV2 Rep gene sequence in pXR2 via SacI and SacII restriction sites.

Production of rAAV. Recombinant AAV vectors were generated using HEK293 cells grown under serum-free suspension conditions in shaker flasks (J. Grieger et al., unpublished data). The suspended HEK293 cells were transfected using polyethyleneimine (PEI; Polysciences), plasmids pXX680 and pXR2, and a vector genome plasmid. At 48 h posttransfection, cell cultures were collected into 500-ml polypropylene conical tubes (Corning) and centrifuged at 655 × *g* for 10 min using a Sorvall RC3C plus centrifuge and H6000A rotor. The supernatant was discarded, and the cells were suspended in a total volume of ~7 ml with H_2O, sonicated, and purified over a discontinuous iodixanol gradient, followed by passage through a heparin column, as described previously (46). Individual vector preparations were compared against plasmid and/or known virus standards by quantitative PCR to determine the number of vector genomes (vg) per ml.

Vectors packaging self-complementary CMV (scCMV)-eGFP with the AAV serotype 2 capsid and single-stranded CMV (ssCMV)-eGFP with

TABLE 1 Cell lines used in this study

Species and cell line	Mutated protein	Source (reference)
Human		
NHF-hTERT	None	W. K. Kaufmann (48)
ATLD2-hTERT	Mre11	W. K. Kaufmann (48)
AT-hTERT	ATM	W. K. Kaufmann (48)
GK41	ATR	Coriell Institute (49, 60–63)
AG06040	BLM	Coriell Institute (49, 60–63)
AG00780	WRN	Coriell Institute (49, 60–63)
M059J	DNA-PKcs	Coriell Institute (49, 60–63)
AG05012	CSA	Coriell Institute (49, 60–63)
Mouse		
wt	None	J. H. Petrini (50, 64)
ATLD1	Mre11	J. H. Petrini (50, 64)
$Mre11^{+/+}$	None	S. Richard (51)
$Mre11^{RK/RK}$	Mre11 GAR domain	S. Richard (51)
$Mre11^{Cond/+}$	None	D. O. Ferguson (52)
$Mre11^{Cond/-}$	Mre11 knockout	D. O. Ferguson (52)
$Mrell^{Cond/H129N}$	Mre11 H129N	D. O. Ferguson (52)

the AAV serotype 1, 3, 4, 5, 6, 8, or 9 capsid were obtained from the University of North Carolina Vector Core Facility. The Ad5-CMV-Cre vector was obtained from the Baylor University Vector Development Lab.

Cell lines and culturing. All cell lines used in this study were cultured at 37°C in 5% CO_2 and grown in a base medium of Dulbecco modified Eagle medium (DMEM; 4.5 g/liter glucose, L-glutamine, sodium pyruvate; Cellgro) supplemented with 10% fetal bovine serum (FBS; Invitrogen), 100 U/ml penicillin, and 100 μg/ml streptomycin (Gibco), modified as indicated below. The human cell lines used in this study were obtained from the Coriell Institute (Camden, NJ), unless otherwise indicated (Table 1) (47). Normal human fibroblasts (NHFs) and AT (with a mutation in ATM) and ATLD2 (with a mutation in Mre11) human fibroblasts immortalized with human telomerase reverse transcriptase (h-TERT) were obtained from W. Kaufmann (University of North Carolina). HeLa and M059J (a glioblastoma with a mutation in the DNA-PK catalytic subunit [DNA-PKcs]) cells, as well as NHFs and AT and ATLD2 human fibroblasts immortalized with h-TERT, were cultured in the base medium (48). Human fibroblast cell line AG00780 (with a mutation in Werner's syndrome helicase [WRN]) was maintained in base medium modified to contain 1× nonessential amino acids (NEAA; Gibco). Human fibroblast cell lines AG06040 (with a mutation in Bloom's syndrome helicase [BLM]) and AG05012 (with a mutation in CSA) were maintained in base medium modified to contain 15% FBS and 1× NEAA. Human osteosarcoma cell line GK41 (which conditionally expresses dominant negative ATR) was maintained in base medium modified to contain 200 μg/ml G418 and 200 μg/ml hygromycin B (49). Expression of ATR kinase dead (ATR-kd) was induced by addition of doxycycline to 1 μg/ml to the cell culture medium beginning 48 h prior to treatment with vectors.

Mouse embryonic fibroblast (MEF) lines with mutations in the Mre11 gene were generously provided by other investigators. MEFs carrying the ATLD1 mutation (a kind gift of J. H. Petrini) and MEFs carrying an arginine-to-lysine (RK) mutation ($Mre11^{RK/RK}$; a kind gift of S. Richard), as well as their isogenic wild-type controls, wt and $Mre11^{+/+}$, respectively, were maintained in the base medium described above (50, 51). MEFs carrying an H129N substitution mutation in the presence of a conditional wt (Cond) allele, as well as deficient and wt controls ($Mre11^{Cond/H129N}$, $Mre11^{Cond/-}$, $Mre11^{Cond/+}$; kind gifts of D. Ferguson) were maintained in base medium modified to contain 10 mM HEPES (Cellgro) and 1× NEAA (52).

Transfection and transductions. In all experiments, cells were counted on a ViCell cell counter (Beckman Coulter) and plated at a known concentration.

For transfection, plasmid DNA (50 ng to 1 μg) was brought to 200 μl with DMEM (without FBS, penicillin, or streptomycin), mixed with 5 to 10 μl of PEI (1 mg/ml) by vortexing, and incubated at ambient temperature (~25°C) for 10 min. This solution was added directly to the growth medium on plated cells at 37°C. After 3 h, medium containing the transfection solution was replaced with growth medium and the cells were cultured until collection at 24 h.

For transduction, viral vectors were diluted in fresh growth medium and exchanged for growth medium on plated cells. AAV vectors were diluted to ~1,000 to 20,000 vg/cell, depending on the cell line, and the Ad vector was diluted to ~2,000 or 8,000 particles/cell. Transduction medium was kept on the cells for 6 h, after which it was replaced with growth medium. Cells were pretreated with ssCMV-E1B55k and scCMV-E4orf6 in a ratio of 1:1 to 1:4 (optimized with each preparation of vector) or an equal concentration of ssCMV-Luc or ssCBA-Luc. Medium containing reporter vector ssCMV-GFP or scCMV-GFP was then added to the cells 18 h after the pretreatment vectors had been removed. This transduction medium was exchanged for growth medium after 6 h. Cells were collected at 24 h after treatment with the reporter vector (Fig. 1B).

Green fluorescent protein (GFP) fluorescence was measured by flow cytometry on a Cyan ADP flow cytometer (Beckman Coulter). The threshold for a positive signal was defined for each cell line as the level of fluorescence above which ~0.5% of untreated cells are counted. The concentration (vg/cell) of GFP reporter vector used with each cell line was adjusted to produce ~1 to 10% GFP-positive cells in luciferase-treated controls. An exception to this was the transduction of HeLa cells with the ssCMV-GFP vector encapsidated by different serotype nucleocapsids, several of which transduced <1% of cultured cells in the absence of E1B55k/E4orf6 (see Fig. 3A).

Antibodies and immunoblotting. Protein levels in total cell lysate were detected by immunoblotting. Cells were lysed with 100 μl of radioimmunoprecipitation assay buffer (25 mM Tris-HCl, pH 7.6, 150 mM NaCl, 1% NP-40, 1% sodium deoxycholate, 0.1% SDS). Lysate was mixed with 1 μl DNase, and this mixture was brought to 1× with Halt protease inhibitor cocktail (Thermo Scientific). Equal fractions of the samples were mixed with 4× sample loading buffer, boiled for 5 to 10 min, resolved by SDS-PAGE, and transferred to a nitrocellulose membrane. Membranes were blocked in 5% bovine serum albumin (BSA) for 1 h at ambient temperature. Adenovirus proteins were detected with the primary antibodies mouse (Ms) anti-E1B55k (2A6; a kind gift from P. Branton) at 1:5,000 and rabbit (Rb) anti-E4orf6 (a kind gift from G. Ketner) at 1:1,000. Cellular proteins were detected with the primary antibodies Rb anti-Mre11 (catalog number 4895; Cell Signaling Technology) at 1:1,000, Rb anti-Nbs1 (catalog number NB100-143; Novus Biologicals) at 1:1,000, and Ms anti-β-actin (catalog number 8226; Abcam) at 1:5,000. Secondary anti-Ms and anti-Rb antibodies conjugated with horseradish peroxidase (HRP) were used at 1:20,000, and goat anti-Ms or anti-Rb antibodies conjugated with IRDye800 or IRDye680 (catalog numbers 926-68070, 926-32210, 926-68021, and 926-32211; LiCor) were used at 1:10,000. Antibody incubations were performed in 1% BSA for 1 h at ambient temperature. Membranes were washed 5 times with TBS-T (50 mM Tris, 150 mM NaCl, 0.05% Tween 20) after incubation with antibody. For visualization of HRP activity, membranes were treated with SuperSignal West Pico chemiluminescent substrate reagents per the manufacturer's instruction (Thermo Scientific). For visualization of the IRDye fluorophores, the membranes were dried and imaged on an Odyssey scanner (LiCor).

Southern blotting. Viral DNA was isolated from cells by a modified Hirt extraction method. Cells were suspended in 259 μl Hirt solution (10 mM Tris-HCl, pH 7.5, 10 mM EDTA). This solution was brought to 0.6% SDS and 1 M NaCl in a total volume of 350 μl. The sample was then mixed and incubated at 4°C for ≥24 h. Precipitated material was pelleted at 16,000 × *g* for 20 min at 4°C. The supernatant was extracted with 350 μl phenol-chloroform-isoamyl alcohol (25:24:1). DNA was precipitated from the aqueous layer after addition of 1 μg glycogen, NaCl to a final concentration of 0.2 M, and 2.2× volumes of ethanol (EtOH). After pel-

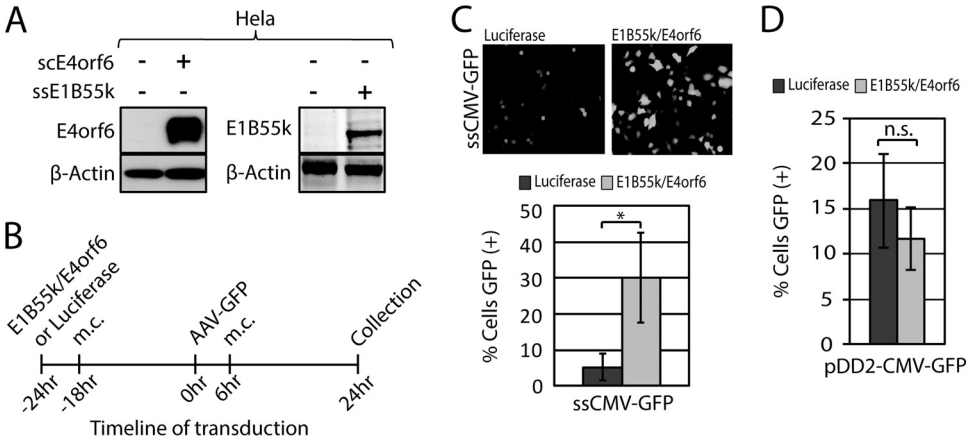

FIG 1 Mobilization of E1B55k/E4orf6 enhancement of AAV gene expression. (A) Expression of Ad proteins E1B55k and E4orf6 from AAV vectors in HeLa cells. Cells received 1,000 vg/cell of the scCMV-E4orf6 or ssCMV-E1B55k vector. Expression of protein was detected in total cell lysate by SDS-PAGE and immunoblotting. The level of β-actin was evaluated as a loading control. (B) Schematic of pulse infection method used to assess the effect of E1B55k/E4orf6 on gene expression from a GFP reporter vector. m.c., medium change. (C) Visualization of GFP expression in transduced cell cultures and quantification of the percentage of cells positive for GFP by flow cytometry. HeLa cells were pretreated to express E1B55k/E4orf6 or luciferase (a total of 2,000 vg/cell) and secondarily transduced with an ssCMV-GFP reporter plasmid (1,000 vg/cell). After 24 h, cells were collected and GFP expression was quantified by flow cytometry. (D) Effect of E1B55k/E4orf6 on transfected plasmid DNA. Cells were pretreated with E1B55k/E4orf6 or luciferase as described in the legend to panel C but secondarily transfected with a plasmid DNA carrying the CMV-GFP expression cassette. Again, GFP expression was quantified by flow cytometry. Error bars represent standard deviations. *, $P < 0.05$; n.s., not significant.

leting at 16,000 × *g* for 10 min, the DNA was washed with 70% EtOH and suspended in 20 μl TE (Tris-EDTA) buffer. The resulting samples were electrophoresed through a 1% agarose gel in TAE buffer (40 mM Tris-acetate, 1 mM EDTA, pH 8.3). The gels were soaked for 15 min in 0.4 N NaOH, 1 M NaCl and transferred to a Hybond-XL membrane (GE Healthcare). The membranes were rinsed in H_2O and then cross-linked with UV. Prehybridization blocking was performed in Church buffer (0.5 M $NaPO_4$, pH 7.5, 1% BSA, 1 mM EDTA, 7% SDS) for ≥30 min at 65°C. Radiolabeled probe was synthesized with a Random Primed DNA labeling kit (Roche) using the AgeI-NotI restriction fragment of pTR2-CMV-GFP-Neo containing only the GFP gene as the template. Purified probe was mixed with 1 mg salmon sperm DNA (Invitrogen), and the mixture was boiled for 5 min prior to addition to the membrane and incubation at 65°C for ~24 h. The membrane was then washed 3 times in high-salt solution (2× SSC [1× SSC is 0.15 M NaCl plus 0.015 M sodium citrate], 0.1% SDS) and once in low-salt solution (0.1× SSC, 0.1% SDS) before exposure to a storage phosphor screen and detection on a Typhoon scanner (GE Healthcare). Densitometric quantitation was performed with ImageQuant software (GE Healthcare).

Fluorescence microscopy. For visualization of the vector, HeLa cells were grown on glass coverslips in 12-well plates. Transduction was conducted as described above. Cells received the E1B55k/E4orf6- or the luciferase-expressing vector at 2,000 vg/cell, and the medium was changed at 6 h. Highly pure Cy5-labeled ssTR2-CMV-GFP-Neo vector (kind gift from P. Xiao) was delivered to the cells 18 h after the pretreatment medium was removed (53). At 6 h postransduction with labeled vector, the coverslips were washed three times with 1× phosphate-buffered saline (PBS), incubated with freshly prepared 2% paraformaldehyde for 15 min, washed three times in 1× PBS again, and mounted onto slides with ProLong Gold antifade reagent with DAPI (4′,6-diamidino-2-phenylindole; Molecular Probes). Cells were imaged on an Odyssey IX81 inverted light microscope.

Statistical analysis. Statistical comparisons were performed using the Wilcoxon signed-rank test between paired data samples. Paired data samples were defined as samples treated, isolated, and analyzed at the same time.

RESULTS

Mobilization of E1B55k/E4orf6 helper function in rAAV vectors. Ad proteins E1B55k and E4orf6 are required for productive infection with AAV during coinfection of these viruses and sufficient for enhancement of gene expression from rAAV vectors. These functions have been linked to degradation of the cellular MRN complex, which poses a severe block to AAV transduction (16). We generated rAAV vectors carrying E1B55k and E4orf6 and rAAV vectors carrying ssCMV-E1B55k and scCMV-E4orf6 in order to facilitate the expression of these proteins in cell lines refractory to other methods of gene transfer (i.e., transfection of plasmid DNA or transduction with lentiviral vectors). Expression of the E1B55k and E4orf6 proteins from these vectors was detected in HeLa cells 24 h after transduction with 1,000 vg/cell by immunoblotting (Fig. 1A). Enhancement of secondary transduction with rAAV was tested for using a pulse infection approach (Fig. 1B). Cells were pretreated with ssCMV-E1B55k/scCMV-E4orf6 or a negative-control vector expressing luciferase for 6 h, after which the medium was replaced. Cells were secondarily treated with the ssCMV-GFP vector 18 h later, and the medium was again replaced after 6 h. This allowed expression of E1B55k/E4orf6 for up to 24 h prior to introduction of the reporter vector. In HeLa cells, pretreatment vectors were delivered at 2,000 vg/cell (total) and the reporter vector was delivered at 1,000 vg/cell. Similar to previous reports, enhancement of gene expression was observed (Fig. 1C). The percentage of cells that scored positive for GFP by flow cytometry was increased ~6-fold ($P < 0.05$). To verify that this enhancement was specific for rAAV vector transduction and not generalized to the CMV promoter or other features of the expression cassette, a control experiment was performed with the transfection of plasmid DNA. No increase in expression was observed with pDD2-CMV-GFP, which carries the same expression cassette as ssCMV-GFP (Fig. 1D). Thus, this method reproduces the helper function of E1B55k/E4orf6 on AAV transduction. Addi-

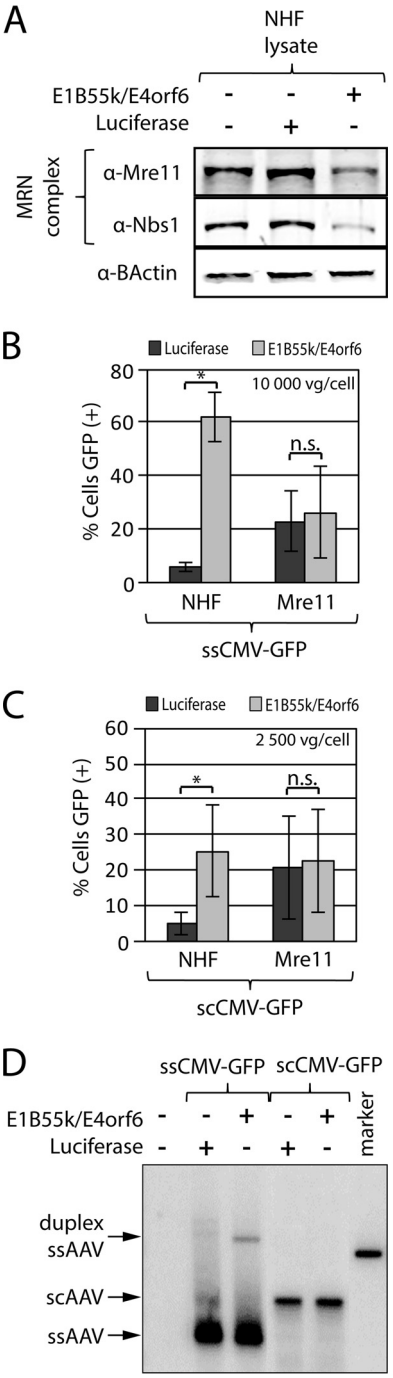

FIG 2 Enhancement of transduction of single-stranded and self-complementary AAV vectors upon degradation of MRN by E1B55k/E4orf6. (A) NHFs were transduced with vectors expressing E1B55k and E4orf6 or luciferase, as a control. Total cellular protein was prepared and analyzed for the levels of the Mre11 and Nbs1 proteins, components of the cellular MRN complex, by SDS-PAGE and immunoblotting. Detection of β-actin served as a loading control. (B and C) Effect of E1B55k/E4orf6 on transduction of single-stranded and self-complementary CMV-GFP reporter vectors, respectively, in normal and Mre11-deficient fibroblasts. NHFs and ATLD2 cells were pretreated to express E1B55k/E4orf6 or luciferase and secondarily transduced with an ssCMV-GFP or scCMV-GFP reporter vector. The level of fluorescence was measured by flow cytometry, and the bar graph shows the percentage of cells positive for GFP. Error bars represent standard deviations. (D) Forms of single-stranded and self-complementary AAV genomes in E1B55k/E4orf6- and luciferase-treated NHFs. AAV genomes were isolated from NHFs by a modified Hirt extraction method and detected by Southern blotting. Radiolabeled probe was generated using the GFP-coding sequence as the template. Blots were detected by storage phosphor imaging and quantitated using ImageQuant software. Molecules that correspond in size to that of the ssCMV-GFP vector (3,381 bp) single-stranded and duplex forms and the scCMV-GFP vector (2,185 bp) duplex form were detected. The marker is a linear restriction product (3,091 bp) containing all of the ssCMV-GFP vector genome except the ITRs. *, $P < 0.05$; n.s., not significant.

tionally, the two-vector approach is efficient enough to affect ≥25% of HeLa cells, which is sufficient to track the effect.

Both single-stranded and double-stranded forms of rAAV are inhibited by MRN. One rationale for mobilizing E1B55k and E4orf6 in rAAV vectors was to study the effect of these proteins in cell lines refractory to other methods of gene transfer. For example, the ability to transduce fibroblasts opens the door to track the enhancement of rAAV in a variety of genetic backgrounds, including patient- and mouse model-derived cell lines. To assess the E1B55k/E4orf6 helper function in such cell lines, we repeated the experimental format performed with HeLa cells outlined in Fig. 1 with an NHF line which has been immortalized with h-TERT (48). A pretreatment vector dose of ~20,000 vg/cell and a secondary treatment dose of ~10,000 vg/cell were used and produced ~2 to 8% GFP-positive cells among control treated cells. Consistent with previous reports, upon delivery of E1B55k/E4orf6, we observed the depletion of the Mre11 and Nbs1proteins of the MRN complex at 24 h postransduction (Fig. 2A). Mre11 and Nbs1 protein levels were not completely degraded, but this was expected due to the efficiency of transduction of this two-vector approach. As was observed with HeLa cells, transduction of ssCMV-GFP was dramatically enhanced in cells expressing E1B55k/E4orf6 compared with the level of transduction in those expressing luciferase (Fig. 2B). At 24 h postransduction, the percentage of cells positive for GFP was increased >10-fold ($P < 0.05$), as measured by flow cytometry, and the effect reached >50% of cells. Enhancement was not observed in the ATLD2 cell line, which has a mutation in Mre11. ATLD2 cells carry a premature stop codon in the gene encoding Mre11 and express a truncated form of the protein (48, 54). Mre11, Rad50, and Nbs1 protein levels and MRN complex formation are reduced in this cell line. The percentage of cells positive for GFP was increased among control-treated ATLD2 cells relative to that among control-treated NHFs (~4-fold), which indicates increased permissiveness to rAAV transduction. The level did not reach that observed with E1B55k/E4orf6-treated NHFs. The reason for this is unclear, but the different genetic backgrounds (ATLD2 and NHF cells are derived from patient fibroblasts and not isogenic) and, possibly, the upregulation of compensatory pathways in ATLD2 cells may play a role. No enhancement was observed in the presence of E1B55k/E4orf6 (Fig. 2B). This finding indicates that the enhancement of gene expression from rAAV by E1B55k/E4orf6 is mediated largely through removal of the block imposed by MRN.

The mechanism through which MRN inhibits AAV is not known, but it affects the transduction of single-stranded vectors prior to completion of second-strand DNA synthesis (16, 35, 36). The pervading model predicts that MRN blocks AAV transduction at the step of second-strand DNA synthesis. The primary evidence for this model is an increase in the completion of double-stranded DNA genomes in the presence of E1B55k/E4orf6 (35, 36). However, this result cannot exclude the possibility that MRN

blocks transduction at a step prior to second-strand DNA synthesis. To resolve this question, we tested whether degradation of MRN by E1B55k/E4orf6 enhances an rAAV vector that does not require DNA synthesis for gene expression. The genome of self-complementary AAV (scAAV) vectors has a central defective ITR flanked by complementary arms of the expression cassette and wild-type ITRs on the ends (55). These molecules can self-anneal immediately upon release into the nucleus and do not require DNA synthesis for expression of the transgene. As a result, scAAV vectors have significantly increased transduction compared with single-stranded AAV (ssAAV). Using the method described above, NHFs and ATLD2 cells were pretreated for expression of E1B55k/E4orf6 or luciferase prior to secondary transduction with scCMV-GFP at a dose of 2,500 vg/cell (which produced ~1 to 10% GFP-positive cells among the luciferase-treated controls). Similar to the result obtained with ssCMV-GFP, the percentage of cells positive for GFP was increased (>5-fold; $P < 0.05$) among NHFs expressing E1B55k/E4orf6 compared with that among NHFs expressing luciferase (Fig. 2C). Again, the effect was not observed in ATLD2 cells.

To evaluate rAAV DNA synthesis, vector genomes were recovered from NHFs by a modified Hirt extraction method and analyzed by Southern blotting with a GFP-specific probe. Analysis of cells receiving ssCMV-GFP revealed an increase in the number of molecules that migrate near the position of the double-stranded vector genome (~3,382 bp), which is indicated by a marker for the vector genome produced by restriction of the vector plasmid (Fig. 2D). Migration to this position is indicative of molecules that have completed second-strand synthesis. The level of these double-stranded genomes was increased ~3-fold in cells expressing E1B55k/E4orf6 (31 ± 13 molecules/cell) compared with that in cells expressing luciferase (12 ± 8 molecules/cell), when measured by densitometric analysis. In contrast, the level of total cell vector genomes remained similar in both treatments (93% ± 9%). Analysis of cells receiving scCMV-GFP revealed molecules that migrate at a position indicative of the self-annealed duplex genome (~2,305 bp) (Fig. 2D). No species with a molecular weight higher than this were observed. Similar to the findings for cells receiving ssCMV-GFP, the level of total cell vector genomes was similar in both treatment groups (~112% ± 23%).

These data demonstrate that the mechanism of MRN inhibition affects both ssAAV and scAAV vectors. Thus, inhibition can occur independently of the requirement for second-strand DNA synthesis.

Inhibition of rAAV by MRN takes place posttrafficking to the nucleus. The observation that the degradation of MRN with E1B55k/E4orf6 enhances both ssAAV and scAAV vectors prompted investigation of steps in transduction prior to second-strand DNA synthesis. Beginning with viral entry, we assessed whether steps early in transduction were impeded by MRN. Vectors encapsidated with different AAV serotype capsid proteins utilize different cell surface receptors for binding and entry (56). To test whether the effect of MRN occurs at these early steps, HeLa cells were treated to express E1B55k/E4orf6 or luciferase (2,000 vg/cell total) and subsequently transduced with rAAV vectors encapsidated with the serotype 1, 3, 4, 5, 6, 8, or 9 capsid protein (1,000 vg/cell). Each vector carried the same ssCMV-GFP expression cassette present in the AAV serotype 2 capsid used in the assays whose results are presented in Fig. 1 and 2. The level of transduction of all serotypes was increased in the presence of E1B55k/E4orf6 compared with that in control cells, indicating that all were subject to inhibition by MRN independently of the surface receptor (Fig. 3A).

Subsequent to binding and entry, AAV is transported via an endocytic pathway to the perinuclear region, where it escapes the endosome and shuttles to the nucleus. This process includes many steps but can be assessed by direct visualization of labeled virus particles (53). To determine whether degradation of MRN affects this transport, the intracellular localization of ssCMV-GFP labeled with the fluorochrome Cy5 was visualized at 6 h postransduction in HeLa cells pretreated to express E1B55k/E4orf6 or luciferase (Fig. 3B). This time point was chosen because previous findings indicated that ~25% of rAAV particles have reached the nucleus at 6 h postransduction and we expected particles to be distributed across all steps of transport leading up to nuclear entry (53). Upon visualization, the distribution of Cy5-ssCMV-GFP was similar in cells expressing E1B55k/E4orf6 or luciferase and typified the pattern previously reported for rAAV. Viral particles appeared across the cytoplasm but were concentrated at a perinuclear site in the cell. Trafficking of rAAV has been shown to involve the microtubule network, and this perinuclear site colocalizes with the microtubule organization center (53). We did not observe a relocalization of the vector to suggest that trafficking was significantly altered in a way that might account for the >10-fold increase in transduction. Instead, these data suggest that the mechanism of inhibition of rAAV by MRN occurs posttrafficking to the nucleus.

MRN inhibits the transduction of rAAV vectors independently of several key downstream DNA damage response factors. The roles of the MRN complex include sensing of DNA damage and activation of downstream signaling kinases, which in turn initiate DDR (18, 19, 57). One of the primary targets for activation by MRN, ATM kinase, has previously been shown to limit the transduction of both ssAAV and scAAV vectors (58, 59). Thus, it is possible that inhibition of rAAV by MRN is mediated through downstream signaling and/or DNA repair factors. To determine if this is the case, we tested whether the degradation of MRN by E1B55k/E4orf6 results in the increased transduction of rAAV in a panel of cell lines mutated for downstream signaling and repair factors. The cell lines tested were deficient for key signaling kinases, ATM and ATR, as well as repair factors Bloom's syndrome helicase (BLM), which is involved in HR repair; Werner's syndrome helicase (WRN) and DNA-PKcs, which are involved in NHEJ repair; and CSA, which is involved in nucleotide excision repair (NER) (48, 49, 60–63). As in the assay whose results are presented in Fig. 1, cells were pretreated to express E1B55k/E4orf6 or luciferase and subsequently transduced with the ssCMV-GFP or scCMV-GFP reporter vector. The dose of vector used with each cell line was selected to produce ~1 to 5% GFP-positive cells among control cells expressing luciferase. GFP expression was measured at 24 h by flow cytometry. An increase in the percentage of cells positive for GFP was observed with both vectors in all cell lines when E1B55k/E4orf6 was expressed compared to the percentage observed when the luciferase control was expressed (Fig. 4). Thus, inhibition of rAAV is intact in each of these cell lines and, therefore, independent of the mutated protein. Differences in the scale of the effect were observed between several of the cell lines. Cell lines defective for ATM, ATR, and WRN exhibited increases in transduction of ~3- to 5-fold for the scCMV-GFP vector and ~5- to 8-fold for the ssCMV-GFP vector. In contrast, cell lines

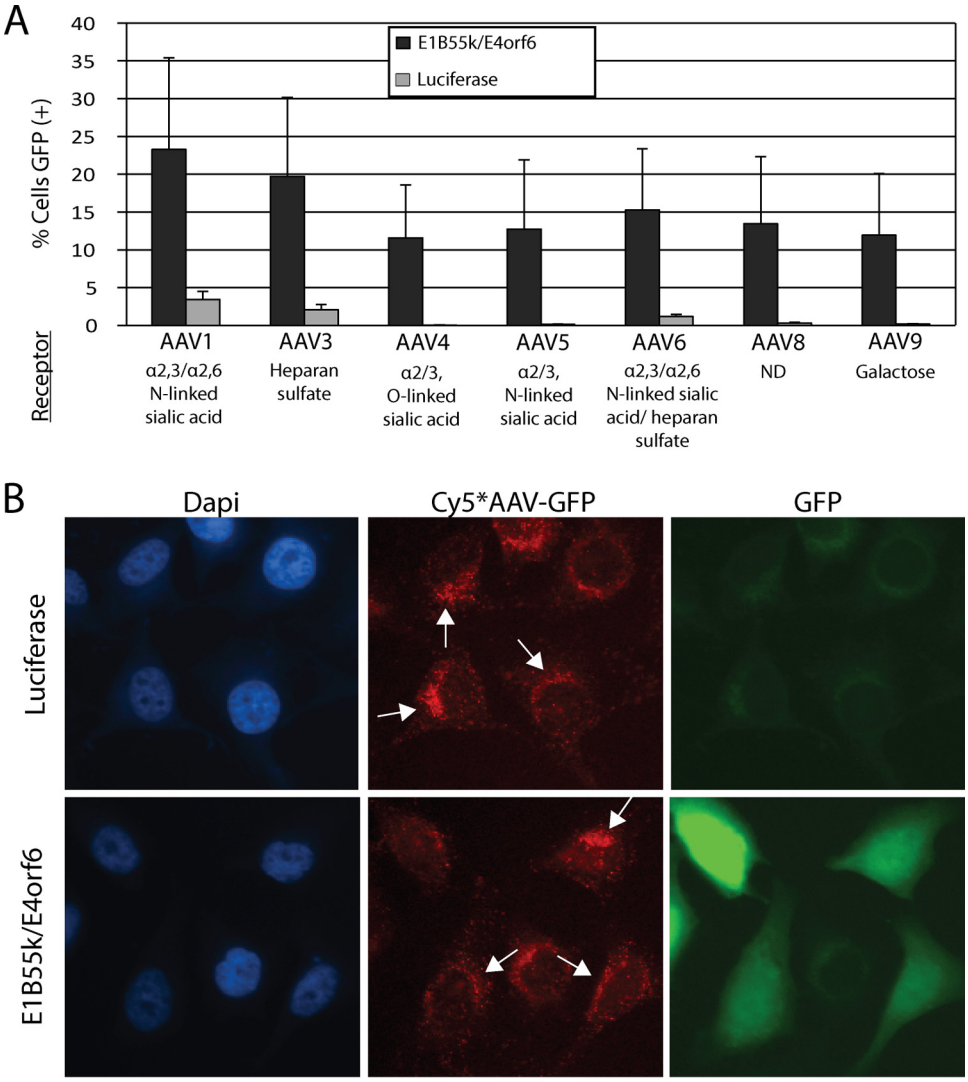

FIG 3 Effect of degradation of MRN on early steps in transduction of AAV. (A) HeLa cells were pretreated to express E1B55k/E4orf6 or luciferase (2,000 vg/cell total) and subsequently transduced with AAV vectors encapsidated with the capsid of the indicated serotype (10,000 vg/cell). Each vector packages the same genome (CMV-GFP) but differs in the cell surface receptor used (indicated below the graph). Expression of GFP was quantified by flow cytometry. The differences between E1B55k/E4orf6- and luciferase-treated samples were statistically significant ($P < 0.05$) for all serotypes. ND, not determined. (B) HeLa cells, pretreated as described in the legend to panel A, were subsequently transduced with the ssCMV-GFP vector encapsidated with the serotype 2 capsid protein and conjugated with the fluorophore Cy5 (1,000 vg/cell). At 6 h postransduction with the labeled vector, cells were fixed and mounted onto slides. Cy5 and GFP were visualized directly by fluorescence microscopy. Nuclei were detected by DAPI staining. The perinuclear accumulation of Cy5 label is indicated (arrows). Error bars represent standard deviations.

defective for BLM, DNA-PKcs, and CSA exhibited a scale of increase more similar to that observed with normal fibroblasts: ~8- to 9-fold for scCMV-GFP and ~10- to 15-fold for ssCMV-GFP. The ability to draw conclusions from these differences is complicated by the fact that the cell lines are not isogenic and subject to different genetic backgrounds, which may modify the scale of the effect. However, it is worth noting that ATM and ATR have been shown to negatively affect gene expression from rAAV. The reduced effect of MRN in cell lines deficient for these factors may reflect a contribution of ATM and ATR. Interestingly, our results indicate that WRN may make a similar contribution to the inhibition of gene expression from rAAV.

DNA binding activity appears to be more important than the nuclease activity of Mre11 for inhibition of rAAV by MRN. The finding that the mechanism of inhibition of rAAV transduction by MRN is independent of downstream signaling and repair factors turned our attention to the activities of the complex itself. Several functions of the MRN complex can be attributed to subunit proteins and, in some cases, distinct domains mapped within those proteins. Two critical activities, DNA binding and nuclease activities, have been linked to defined domains on the Mre11 protein (Fig. 5A) (19, 51, 52). In order to evaluate whether inhibition of rAAV requires either of these activities, vector transduction was evaluated in the presence of specific mutations in these domains. For comparison with isogenic wt controls, we were interested in studying these mutations in the context of fibroblasts derived from transgenic mouse cell lines (MEFs), so we first tested for conservation of MRN inhibition of rAAV in mouse cells. To do

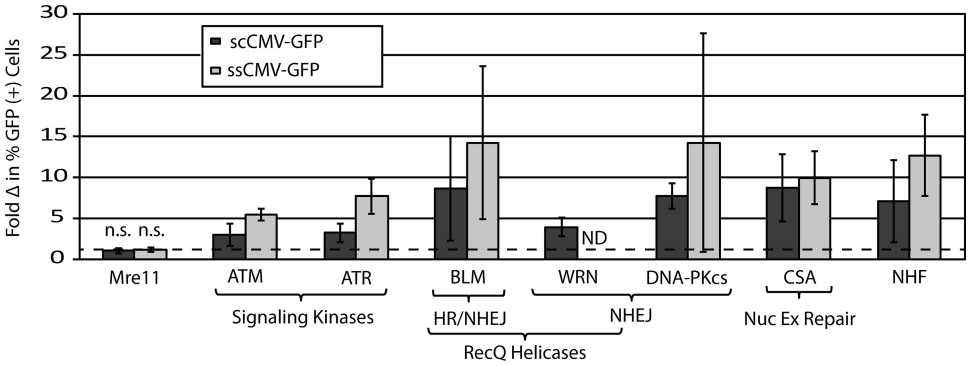

FIG 4 Effect of degradation of MRN on transduction of AAV in cell lines deficient for DNA damage signaling and repair factors. Cell lines defective for ATM (AT), ATR (GK41), BLM (AG06040), WRN (AG00780), DNA-PKcs (M059J), or CSA (AG05012) were tested for enhancement of AAV transduction upon degradation of MRN by E1B55k/E4orf6. Cells were pretreated to express E1B55k/E4orf6 or luciferase and subsequently transduced with ssCMV-GFP or scCMV-GFP reporter vector. The amount of vector used (vg/cell) was determined for each cell line, and ~1 to 10% GFP-positive cells were produced among luciferase-treated control cells. GFP fluorescence was measured by flow cytometry, and the percentage of cells positive for GFP was determined. The fold change (Δ) in the percentage of GFP-positive cells was calculated by dividing the percentage of GFP-positive cells among E1B55k/E4orf6-treated cells by the percentage of GFP-positive cells among luciferase-treated cells. Error bars represent standard deviations. The fold difference between E1B55k/E4orf6- and luciferase-treated samples was statistically significant ($P < 0.05$), unless otherwise indicated. ND, not determined; n.s., not significant.

this, the transduction of scAAV-GFP was compared in MEFs carrying an A-to-T substitution at nucleotide 1894 of the mouse Mre11 gene (50, 64). This mutation results in a 75-amino-acid truncation of the protein and is analogous to human ATLD1 and ATLD2 mutations (a C-to-T substitution at nucleotide 1897). Expression of GFP was increased >2-fold ($P < 0.05$) in the ATLD1 cells compared with that in the wt controls (Fig. 5B). The degree of the effect was not as great as that observed in human cells, but it confirms Mre11 inhibition of rAAV in mouse cells.

To assess the contribution of the functional domains of Mre11, transduction of rAAV was measured in MEFs with a mutation in the glycine-arginine-rich (GAR) motif within the DNA binding

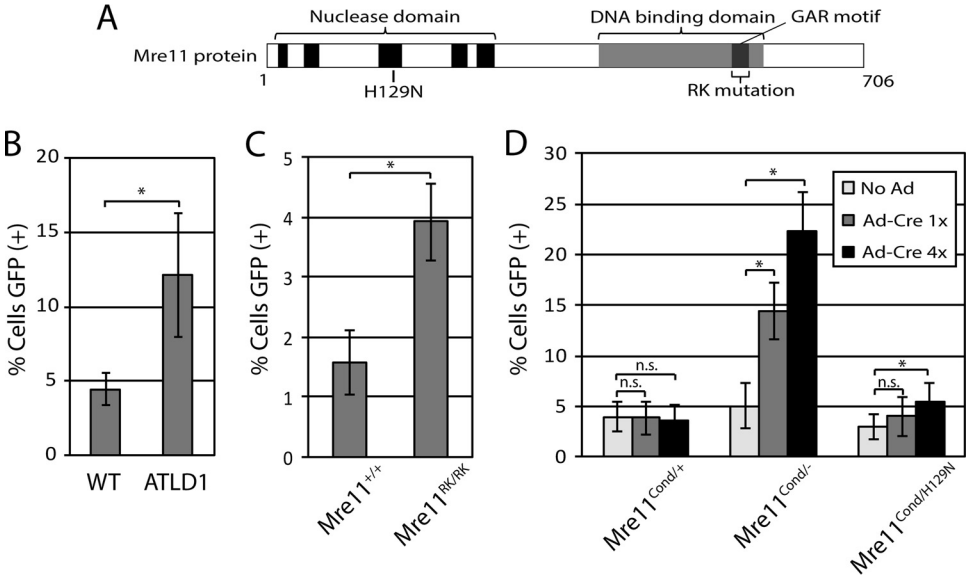

FIG 5 Role of the functional domains of the Mre11 protein in inhibition of transduction of AAV. (A) Schematic of the spatial arrangement of functional domains on the Mre11 protein (706 amino acids). The nuclease domain is comprised of five motifs located near the amino terminus of the protein and includes histidine 129, which is required for nucleolytic activity. The DNA binding domain is located near the carboxyl terminus and includes a glycine-arginine-rich (GAR) domain, which is a preferred site of protein methylation. The positions of the H129N and RK mutations are indicated. (B) Transduction of MEFs deficient for Mre11. MEFs (ATLD1 cells) carrying a mutation (premature stop codon) that mimics the human ATLD2 mutation (Fig. 2) and isogenic wt controls were transduced with the scCMV-GFP reporter vector at a dose of 10,000 vg/cell. Cells were collected at 24 h postransduction, and the percentage of cells positive for GFP was measured by flow cytometry. (C) $Mre11^{RK/RK}$ MEFs, which have the arginine residues of the GAR motif in the DNA binding domain replaced by lysines, and isogenic wild-type ($Mre11^{+/+}$) controls were treated as described in the legend to panel B. (D) $Mre11^{Cond/H129N}$ MEFs have an asparagine substituted for the histidine at amino acid position 129. This mutation is embryonic lethal and is carried in the presence of a conditional wild-type allele. The phenotype of the mutant allele is exposed by Cre-mediated excision of the conditional allele. $Mre11^{Cond/H129N}$ MEFs, as well as wt ($Mre11^{Cond/+}$) and knockout ($Mre11^{Cond/-}$) controls, were transduced with the Ad-Cre vector at 2,000 (1×) or 8,000 (4×) particles/cell to remove the conditional allele. After ~96 h, cells were transduced with the scCMV-GFP vector. The percentage of cells positive for GFP fluorescence was measured by flow cytometry 24 h after delivery of the reporter vector. *, $P < 0.05$; n.s., not significant.

domain of Mre11 (51). GAR motifs are preferred sites of methylation by protein arginine N-methylation (PRMT) enzymes (65). In the mutant $Mre11^{RK}$, nine arginine residues of the Mre11 GAR motif are replaced by lysine. Yu et al. (51) described the interaction between the mutant protein and MRN counterparts Rad50 and Nbs1 and assembly into foci in response to DNA damage. Defects in nuclease activity, DNA binding, ATR/Chk1 activation and signaling, and, to a small degree, class switch recombination (CSR) were reported. ATM/Chk2 activation and signaling were determined to be intact in the presence of this mutation. Transduction of this cell line with scAAV-GFP resulted in an increase in the level of expression of GFP of ~2.5-fold ($P < 0.05$) compared with that by the isogenic wt controls (Fig. 5C), similar to the findings for ATLD mutant MEFs. Thus, one or more of the activities defective in the $Mre11^{RK}$ mutant contributes to inhibition of rAAV transduction.

The mutant H129N substitutes a residue critical for the nuclease activity of Mre11 (52). Amino acid H129 is responsible for stabilizing the scissile phosphate of the DNA backbone during nucleotide excision. Mutation of this residue is embryonic lethal in mice but is maintained in the presence of a conditional wt allele in $Mre11^{Cond/H129N}$ MEFs. Excision by Cre recombinase exposes the mutant phenotype. Buis et al. (52) determined that the $Mre11^{H129N}$ protein is stably expressed, interacts with Rad50 and Nbs1, and assembles in foci at sites of DNA damage. This mutant protein was found to be defective in nuclease activity, ATR/Chk1 activation and signaling, and homologous recombination. Its roles in DNA binding and ATM/Chk2 activation and signaling were intact. To test for inhibition of rAAV, $Mre11^{Cond/+}$, $Mre11^{Cond/-}$, and $Mre11^{Cond/H129N}$ MEFs were treated with Ad-Cre (2,000 or 8,000 particles/cell) in order to excise the conditional allele. The E1 genes are deleted in the Ad5-CMV-Cre vector used for this purpose, and the E1B55k/E4orf6 complex is not intact in this vector. Though this vector expresses E4orf6, this protein alone is insufficient for the degradation of MRN and enhancement of rAAV (data not shown) (16). Cells were secondarily transduced with scCMV-GFP, and transgene expression was measured by flow cytometry (Fig. 5D). The level of GFP expression was increased ~4-fold and ~7-fold ($P < 0.05$) with treatment of 2,000 and 8,000 particles/cell of Ad5-CMV-Cre, respectively, in the $Mre11^{\Delta/-}$ control (Δ indicates removed conditional allele), consistent with the loss of MRN inhibition. No increase was observed in $Mre11^{\Delta/+}$ or $Mre11^{\Delta/H129N}$ cells treated with the lowest dose of Ad5-CMV-Cre. At the highest dose of Ad-CMV-Cre tested, 8,000 particles/cell, a statistically significant ($P < 0.05$) increase was observed in $Mre11^{\Delta/H129N}$ cells, but the increase (<1.5-fold) was less than that observed with the loss of Mre11 ($Mre11^{\Delta/-}$) or mutation of the DNA binding domain ($Mre11^{RK/RK}$, 2.5-fold). These data reveal that inhibition of rAAV by MRN correlates with DNA binding ability more than the nuclease activity of Mre11 does. Additionally, the results corroborate the findings of analysis of human cell lines, in which inhibition was independent of DNA damage factors, including ATM and ATR kinases.

Inhibition of rAAV by MRN is independent of the sequence and host species of the ITR. The results presented above indicate that MRN inhibition of rAAV affects the vector genome specifically and not a plasmid template for expression (Fig. 1D) and requires the DNA binding properties of Mre11. Consistent with this, previous studies have provided evidence for a direct physical interaction between MRN and the AAV genome, possibly mediated through the terminal ITR structure. AAV genomes coprecipitate with Mre11 from cell lysates, and the electromobility of an oligonucleotide representing the AAV ITR is shifted in the presence of the Mre11 and Nbs1 proteins *in vitro* (16, 27). We wanted to determine if a change to the sequence or structural features of the ITR affects MRN inhibition of rAAV. Our group has described ITRs altered in sequence and structure from the serotype 2 ITR that retain the replication and packaging function (43, 66). The ITR of serotype 5 AAV shares only ~57% nucleotide sequence identity with that of AAV2 and also differs in the spacing of terminal and nicking stem-loop structures and overall length (Fig. 6A). Mutants ITR2+5NS and ITR5+2SNS are hybrids of the AAV2 and AAV5 ITRs, respectively, in which the relative position of the spacer region, the terminal stem-loop, and the nicking stem-loop, as well as the sequence of the ITR, has been altered. Vectors carrying these ITRs packaging the CMV-GFP expression construct were evaluated for relative transduction efficiency as well as the level of enhancement upon degradation of MRN by E1B55k/E4orf6 in NHFs (Fig. 6B). Each of these vectors exhibited a reduced transduction efficiency relative to that of wild-type AAV2 ITR in cells expressing the luciferase control (~11-fold for ITR2+5NS, ~5-fold for ITR5+2SNS, and ~4-fold for ITR of AAV5; $P < 0.05$) at a dose of 10,000 vg/cell. However, the level of transgene expression from vectors carrying ITR2+5NS and ITR5+2SNS increased ~55-fold and ~26-fold, respectively, to be near that from vectors carrying ITR2 (within ~1.3-fold) in cells expressing E1B55k/E4orf6 (Fig. 6C). The transduction efficiency of the vector carrying ITR5 increased ~8.9-fold so that it was only within ~2.7-fold of that of the vector carrying ITR2. Thus, the hybrid ITRs experience a greater level of enhancement than either of the wild-type ITRs.

To determine if inhibition by MRN is specific for human AAV serotype ITRs, we developed a vector that has the CMV-GFP expression cassette substituted into snake AAV. This vector carries snake AAV ITR sequences, which have only ~50% nucleotide sequence identity with serotype 2 or 5 ITRs. This vector could be replicated and packaged in HEK293 cells expressing AAV2 and snake AAV Rep and Cap proteins, as well as Ad helper proteins. Transduction of NHFs, pretreated to express E1B55k/E4orf6 or luciferase (2000 vg/cell total), with snake ITR revealed activity similar to that of the AAV5 ITR vector. Expression of GFP was increased >10-fold in cells expressing E1B55k/E4orf6 compared to that in cells expressing luciferase. This indicates that inhibition of rAAV by MRN is not specific to human serotype ITRs but can be generalized to ITRs of different species.

DISCUSSION

It is well established that cellular DDR networks, made up of sensory, signaling, and repair factors, play a central role in the permissiveness of a cell to viral infection (7, 17). Factors of these pathways, which normally function in maintenance of the cellular genome, adopt auxiliary roles in response to invading genetic material. The complex made up of Mre11, Rad50, and Nbs1 (MRN) is critical in this struggle between pathogen and host. In this study, we investigated the mechanism of MRN inhibition of gene expression from recombinant AAV. Recombinant AAV vectors have had AAV genes and promoters removed and, instead, contain reagents currently in clinical development. Thus, the mechanism in question has high therapeutic relevance.

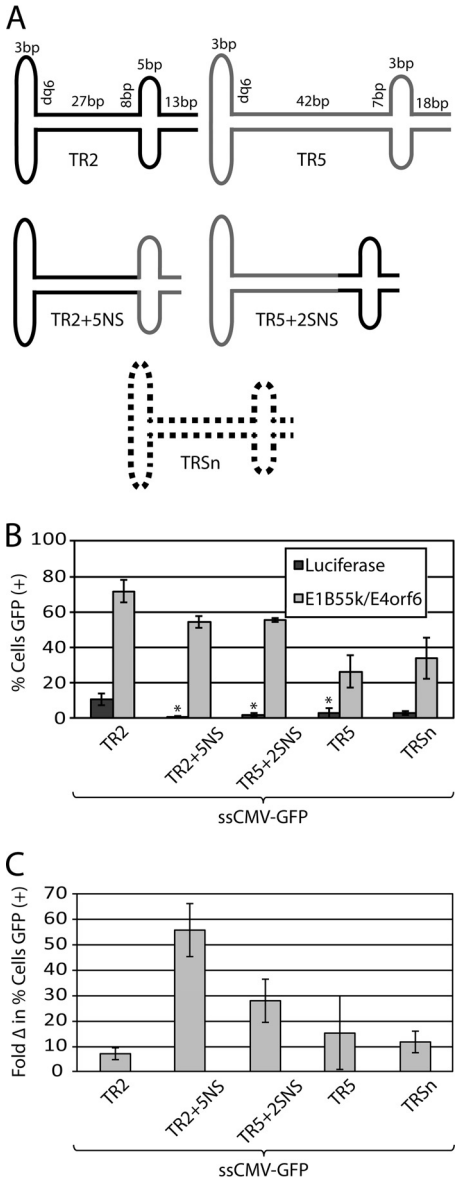

FIG 6 Effect of degradation of MRN on AAV vectors with mutant or nonhuman ITRs. (A) Schematic of wild-type and mutant ITRs. The vectors used in this experiment were flanked by the human AAV serotype 2 ITR (TR2), the human AAV serotype 5 ITR (TR5), transverse chimeras of these two serotypes (TR2+5NS and TR5+2SNS), or serpentine AAV ITR (TRSn). (B) Level of vector transduction. NHFs were pretreated to express E1B55k/E4orf6 or luciferase (20,000 vg/cell total) and secondarily transduced with ssCMV-GFP reporter vectors (10,000 vg/cell) flanked by the indicated ITR. The percentage of cells positive for GFP was measured by flow cytometry. Statistical comparison between TR2+5NS, TR5+2SNS, or TR5 and TR2 was performed. *, $P < 0.05$. (C) Fold change in the percentage of cells positive for GFP.

The mobilization of Ad proteins E1B55k and E4orf6 in rAAV vectors allowed study of the effect of transient degradation of MRN on secondary rAAV transduction in human and mouse fibroblast cell lines, which are refractory to other methods of gene delivery (e.g., transfection of plasmid DNA and transduction of lentivirus). We found that delivery of E1B55k and E4orf6 on separate vectors was efficient enough to reach ~25% of HeLa cells and >50% of NHFs at the doses used (Fig. 1C and 2B) and reproduces the mechanism of enhancement of wt AAV and rAAV reported in previous studies (16, 35, 36). Gene expression from rAAV was increased in both of these cell types: ~5-fold in HeLa cells and ~10-fold in NHFs. The levels of MRN proteins Mre11 and Nbs1 were reduced with treatment with E1B55k/E4orf6, indicating degradation of this complex, and completion of second-strand DNA synthesis was increased with an ssAAV vector in NHFs (Fig. 2A and D). With the ability to track this effect in fibroblasts, we were also able to demonstrate that enhancement of gene expression from rAAV is not observed in patient-derived ATLD2 cells, which are deficient for Mre11 and highly permissive to transduction (Fig. 2B). This provides direct evidence that the effect of E1B55k/E4orf6 on rAAV is mediated primarily through the degradation of MRN and removal of the inhibition imposed by this complex.

The pervading model for this mechanism of inhibition is that MRN inhibits rAAV by blocking second-strand DNA synthesis. The primary evidence for this is the observation that double-stranded forms of ssAAV genomes are increased with the degradation or knockdown of MRN (16, 35, 36). Using expression of E1B55k/E4orf6 as a tool to track inhibition by MRN, we tested whether double-stranded rAAV (scAAV) vectors, which do not require second-strand DNA synthesis for gene expression, are enhanced in a manner similar to that for ssAAV vectors. Our results indicate that MRN inhibits both ssAAV and scAAV (Fig. 2C). Southern blotting to detect vector genomes revealed that, while conversion of ssAAV to the duplex form is increased, scAAV genomes appear in duplex form independently of the degradation of MRN (Fig. 2D). Additionally, higher-molecular-weight species were not detected. These findings are in contrast to the expected result that only ssAAV vectors would be affected if inhibition by MRN were the result of a block to DNA synthesis exclusively. Instead, we can conclude that at least part of the mechanism of inhibition precedes second-strand synthesis and is common to single- and double-stranded templates.

Eliminating a block to second-strand DNA synthesis impelled us to explore other possible mechanisms of inhibition of rAAV by MRN. Inhibition was not observed with the CMV-GFP expression cassette when delivered in the form of a transfected plasmid DNA template, which did not display an increase in gene expression upon degradation of MRN (Fig. 1D). Thus, the possibility of an effect on the promoter, transport of the message, or translation of the protein can be excluded. Testing steps in transduction as early as cell receptor binding and entry, we found evidence that inhibition is independent of cell receptor usage (Fig. 3A) and does not dramatically alter intracellular trafficking of the capsid (Fig. 3B). Therefore, the mechanism of inhibition appears to take place in the nucleus posttrafficking, which is consistent with the known roles of MRN in DNA damage signaling and repair.

In response to sensing damage to the cellular genome, one primary function of MRN is initiation of damage signaling and activation of downstream repair networks (24–26). Previous studies have indicated that signaling kinases ATM and ATR, the primary targets of activation by MRN, can inhibit the transduction of AAV (58, 59). Similarly, ATM is not required for the concatenation of the Ad genome, observed when MRN is intact, but does contribute to the inhibition of gene expression from this virus (32, 67). We investigated whether inhibition of rAAV by MRN involves downstream damage signaling and repair by testing for enhancement with E1B55k/E4orf6 in cell lines deficient for several

DDR factors. Cell lines deficient for ATM and ATR, as well as Bloom's syndrome helicase (BLM; which participates in the HR and NHEJ pathways), Werner's syndrome helicase (WRN; which participates in the NHEJ pathway), DNA-PKcs (which participates in the NHEJ pathway), and CSA (which participates in NER), were assessed. These cell lines were chosen because the mutant factors participate in three separate pathways of DNA damage repair, HR, NHEJ, and NER. In all cell lines, expression of E1B55k/E4orf6 led to the enhancement of transduction of rAAV, indicating that the factors tested are not required for inhibition (Fig. 4). Interestingly, though an increase in the fold change in the percentage of GFP-positive cells of a scale similar to that in NHFs was observed in BLM-, DNA-PKcs-, and CSA-deficient cell lines, enhancement was not as great in cell lines deficient for ATM, ATR, and WRN. Given that kinases ATM and ATR are known to negatively impact AAV, it is possible that the reduced effect in these cell lines reflects a partial contribution of these factors. WRN has not previously been tested for involvement in rAAV transduction. Further testing will be required to determine if this factor does, in fact, play an inhibitory role. Together, these findings indicate that inhibition of rAAV by MRN is not dependent on several key factors of DNA damage repair signaling. However, we cannot eliminate the possibility that other damage response factors in these pathways play a role.

A second possibility for the mechanism of inhibition is degradation of incoming rAAV genomes directly by MRN. Mre11 possesses phosphoesterase and DNA binding domains, and in purified form it exhibits endo- and exonuclease activity and interacts with ssDNA and double-stranded DNA substrates (68–70). We tested whether either of these functional domains contributes to inhibition of rAAV. Analysis of the MEF lines with mutations in the specific activities of Mre11 demonstrated that the nuclease domain of MRN makes only a minor contribution to inhibition (Fig. 5D). This is similar to the observation that the nuclease activity of Mre11 is not required for inhibition of adenovirus (71). Additionally, quantification of vector genomes by densitometric analysis of DNA from Southern blots and separately by quantitative PCR revealed similar copy numbers between enhanced and nonenhanced cultures (Fig. 2D and data not shown). In contrast, the DNA binding ability appears to make a greater contribution to inhibition of rAAV (Fig. 5C). It would be interesting to look at factors involved early during MRN binding to DNA. MdcI is thought to play a role in loading MRN onto a DNA substrate. Though this factor is not essential for MRN interaction and inhibition of adenovirus, it is possible that MdcI plays a role in loading MRN onto the AAV genome (72). Together, these results argue against a mechanism of direct degradation but corroborate previous evidence for an interaction between MRN and the AAV genome (16, 27).

Evidence from this and previous studies suggests that the DNA binding ability of MRN is important for the mechanism of inhibition. Hairpin secondary structures and double-strand-to-single-strand conversions, both present in the AAV ITR, are known substrates for MRN (57). The *in vitro* binding of the Mre11 and Nbs1 proteins of the MRN complex with an oligonucleotide representing the AAV ITR has been demonstrated by gel shift (16). Here, we tested whether the interaction of MRN with rAAV is dependent on the sequence or structural arrangement of the ITR or specific for human AAV ITRs. AAV serotype 2 and 5 ITRs share only ~57% nucleotide sequence identity. Additionally, we developed mutant ITRs, ITR2+5NS and ITR5+2SNS, with sequence transversions between serotype 2 and 5 ITRs which are able to be replicated and packaged (43). These ITRs rearrange the relative position of the sequence and structural features within the two wt ITRs. We found that vectors carrying these ITRs were all enhanced for transduction upon degradation of MRN in the presence of E1B55k/E4orf6 (Fig. 6). Interestingly, the baseline level of expression was reduced for the two transversion mutants, but the scale of enhancement above the baseline was greater than that observed with either parent serotype 2 or parent serotype 5. This suggests that the extent of inhibition by MRN may be reduced with the wild-type ITR relative to that with the mutant ITRs. Determination of whether this is the case will require testing for a direct interaction of MRN with the ITR and comparative analysis between ITRs of different forms. In addition to the human serotypes, we tested whether MRN inhibits a vector carrying a nonhuman ITR derived from snake AAV, which shares only ~50% nucleotide sequence homology with either the serotype 2 or 5 ITR (45). Transduction of this vector was enhanced to an extent similar to that for the other wild-type ITRs. These findings indicate that the effect of MRN is not dependent on the sequence or the strict positioning of the structural features within the ITR and is generalized to nonhuman ITRs. This is consistent with the known function of MRN in the cell, where it must respond to various forms of DNA damage, independently of sequence. Unfortunately, this likely means that inhibition by MRN cannot be circumvented simply by modification of the ITR.

Ad proteins E1B55k and E4orf6 contribute pleiotropic functions to productive infection of AAV. The ubiquitin ligase complex formed by these factors targets cellular proteins, in addition to MRN, for degradation, including the tumor suppressor p53 and DNA ligase IV (73, 74). Though these other proteins play important roles during productive AAV infection, they do not appear to contribute to the inhibition of gene expression studied here. Modulation of p53 is important for regulating apoptosis and cell survival during AAV infection (75–77). However, mutants of E1B55k incapable of degrading p53 retain the ability to degrade MRN and enhance gene expression and replication of AAV, as shown succinctly by Schwartz et al. (16). Consistent with this, we observed enhancement of rAAV upon expression of E1B55k/E4orf6 in cell lines deficient for p53 (U2OS) (data not shown). DNA ligase IV has been implicated in the integration of AAV genomes, but a role in inhibiting gene expression or replication has not been reported (78). A lack of enhancement of rAAV in ATLD2 cells (Mre11 deficient) indicates that if DNA ligase IV plays a role in this effect, it is mediated through MRN. In addition to antagonizing these cellular factors, E1B55k and E4orf6 have been shown to regulate mRNA trafficking during Ad and AAV infection (79–83). Here, we observed no enhancement of gene expression from a transfected plasmid DNA carrying the vector genome or in cell lines deficient for Mre11 (ATLD2) (Fig. 1D and 2B). This effect was observed with non-AAV transcriptional elements [i.e., CMV or the CBA promoter and simian virus 40 poly(A)], so it remains possible that E1B55k/E4orf6 may enhance the expression of AAV promoters or trafficking of viral mRNAs during wt AAV infection. Thus, the effect that we were monitoring here appears to be mediated solely through degradation of MRN.

Together, the findings reported here greatly advance our understanding of the mechanism of inhibition of rAAV by the MRN complex. We have demonstrated that the mechanism is not exclu-

sively a block in second-strand DNA synthesis, as previously proposed, but affects both single- and double-stranded rAAV genomes. We can also rule out a contribution of key downstream DDR factors and degradation of the vector genome as the mechanism of inhibition of gene expression from rAAV by MRN. Instead, our results are consistent with a block to gene expression after trafficking to the nucleus but prior to second-strand DNA synthesis. The details of this mechanism are not resolved and require further investigation. However, we can propose several possible mechanisms based on our observations and previously reported activities of MRN. One model is that interaction with MRN sequesters the rAAV genome to a site within the nucleus inaccessible to cellular factors necessary for gene expression and DNA synthesis (e.g., transcription factors). There is clear evidence for the colocalization of MRN with incoming rAAV genomes soon after transduction (27). Though the location of this interaction has not been compared with that of transcription centers within the nucleus, these sites may be exclusive. A second possibility is that the nature of the interaction of MRN with the rAAV genome poses a steric block to binding of transcription factors. There is evidence that MRN binds the ITR structures present on the ends of the rAAV genome (16). Binding at these structures would place MRN upstream of and in proximity to the promoter for gene expression. Additionally, the structure of MRN allows dimerization between complexes formed at distal sites in the genome via a hook domain in Rad50 (19, 21). During the response to damage to the cellular genome, this function is thought to play a role in maintaining proximity between sister chromatids to facilitate homologous recombination repair and in stabilizing replication fork progression. In the context of interaction with the rAAV genome, dimerization between MRN complexes bound at the ITR within (*cis*) or between (*trans*) genomes may occur. The formation of such structures, albeit speculative, may contribute to reduced gene expression via steric hindrance or another mechanism.

ACKNOWLEDGMENTS

We thank D. Ferguson, S. Richard, and J. H. Petrini for generously providing the MEF lines. We thank P. Hearing for providing the plasmid pCMV-E4orf6 and P. Tijssen for providing the plasmid pSAAV. We thank P. J. Xiao for providing reagents and assistance with microscopy, M. Hirsch for cloning of pdsEMBL-CMV-E4orf6, C. Hewitt for cloning of pTRSn-CMV-eGFP, and J. Grieger for reagents. We thank D. Ornelles for critical review of the manuscript and M. Weitzman for helpful discussion.

This work was supported by National Institutes of Health grants R01AI072176, R01AR064369, R01DK084033, and P01HL1127611 (to R.J.S.) and National Institutes of Health grant T32-CA009156 (to T.B.L.) and received support from the Alpha-1 Foundation (T.B.L.).

REFERENCES

1. **Lusby E, Fife KH, Berns KI.** 1980. Nucleotide sequence of the inverted terminal repetition in adeno-associated virus DNA. J Virol **34:**402–409.
2. **Tattersall P, Ward DC.** 1976. Rolling hairpin model for replication of parvovirus and linear chromosomal DNA. Nature **263:**106–109. http://dx.doi.org/10.1038/263106a0.
3. **Samulski RJ, Chang LS, Shenk T.** 1989. Helper-free stocks of recombinant adeno-associated viruses: normal integration does not require viral gene expression. J Virol **63:**3822–3828.
4. **Srivastava A, Lusby EW, Berns KI.** 1983. Nucleotide sequence and organization of the adeno-associated virus 2 genome. J Virol **45:**555–564.
5. **Nash K, Chen W, Muzyczka N.** 2008. Complete in vitro reconstitution of adeno-associated virus DNA replication requires the minichromosome maintenance complex proteins. J Virol **82:**1458–1464. http://dx.doi.org/10.1128/JVI.01968-07.
6. **Geoffroy MC, Salvetti A.** 2005. Helper functions required for wild type and recombinant adeno-associated virus growth. Curr Gene Ther **5:**265–271. http://dx.doi.org/10.2174/1566523054064977.
7. **Weitzman MD, Lilley CE, Chaurushiya MS.** 2010. Genomes in conflict: maintaining genome integrity during virus infection. Annu Rev Microbiol **64:**61–81. http://dx.doi.org/10.1146/annurev.micro.112408.134016.
8. **Turnell AS, Grand RJ.** 2012. DNA viruses and the cellular DNA-damage response. J Gen Virol **93:**2076–2097. http://dx.doi.org/10.1099/vir.0.044412-0.
9. **Fragkos M, Breuleux M, Clement N, Beard P.** 2008. Recombinant adeno-associated viral vectors are deficient in provoking a DNA damage response. J Virol **82:**7379–7387. http://dx.doi.org/10.1128/JVI.00358-08.
10. **Schwartz RA, Carson CT, Schuberth C, Weitzman MD.** 2009. Adeno-associated virus replication induces a DNA damage response coordinated by DNA-dependent protein kinase. J Virol **83:**6269–6278. http://dx.doi.org/10.1128/JVI.00318-09.
11. **Duan D, Yan Z, Yue Y, Engelhardt JF.** 1999. Structural analysis of adeno-associated virus transduction circular intermediates. Virology **261:**8–14. http://dx.doi.org/10.1006/viro.1999.9821.
12. **McCarty DM, Young SM, Jr, Samulski RJ.** 2004. Integration of adeno-associated virus (AAV) and recombinant AAV vectors. Annu Rev Genet **38:**819–845. http://dx.doi.org/10.1146/annurev.genet.37.110801.143717.
13. **Collaco RF, Bevington JM, Bhrigu V, Kalman-Maltese V, Trempe JP.** 2009. Adeno-associated virus and adenovirus coinfection induces a cellular DNA damage and repair response via redundant phosphatidylinositol 3-like kinase pathways. Virology **392:**24–33. http://dx.doi.org/10.1016/j.virol.2009.06.005.
14. **Choi YK, Nash K, Byrne BJ, Muzyczka N, Song S.** 2010. The effect of DNA-dependent protein kinase on adeno-associated virus replication. PLoS One **5:**e15073. http://dx.doi.org/10.1371/journal.pone.0015073.
15. **Inagaki K, Ma C, Storm TA, Kay MA, Nakai H.** 2007. The role of DNA-PKcs and Artemis in opening viral DNA hairpin termini in various tissues in mice. J Virol **81:**11304–11321. http://dx.doi.org/10.1128/JVI.01225-07.
16. **Schwartz RA, Palacios JA, Cassell GD, Adam S, Giacca M, Weitzman MD.** 2007. The Mre11/Rad50/Nbs1 complex limits adeno-associated virus transduction and replication. J Virol **81:**12936–12945. http://dx.doi.org/10.1128/JVI.01523-07.
17. **Weitzman MD, Weitzman JB.** 2014. What's the damage? The impact of pathogens on pathways that maintain host genome integrity. Cell Host Microbe **15:**283–294. http://dx.doi.org/10.1016/j.chom.2014.02.010.
18. **Assenmacher N, Hopfner KP.** 2004. MRE11/RAD50/NBS1: complex activities. Chromosoma **113:**157–166. http://dx.doi.org/10.1007/s00412-004-0306-4.
19. **Lamarche BJ, Orazio NI, Weitzman MD.** 2010. The MRN complex in double-strand break repair and telomere maintenance. FEBS Lett **584:**3682–3695. http://dx.doi.org/10.1016/j.febslet.2010.07.029.
20. **Rass E, Grabarz A, Plo I, Gautier J, Bertrand P, Lopez BS.** 2009. Role of Mre11 in chromosomal nonhomologous end joining in mammalian cells. Nat Struct Mol Biol **16:**819–824. http://dx.doi.org/10.1038/nsmb.1641.
21. **Stracker TH, Petrini JH.** 2011. The MRE11 complex: starting from the ends. Nat Rev Mol Cell Biol **12:**90–103. http://dx.doi.org/10.1038/nrm3047.
22. **Lukas C, Falck J, Bartkova J, Bartek J, Lukas J.** 2003. Distinct spatiotemporal dynamics of mammalian checkpoint regulators induced by DNA damage. Nat Cell Biol **5:**255–260. http://dx.doi.org/10.1038/ncb945.
23. **Nelms BE, Maser RS, MacKay JF, Lagally MG, Petrini JH.** 1998. In situ visualization of DNA double-strand break repair in human fibroblasts. Science **280:**590–592. http://dx.doi.org/10.1126/science.280.5363.590.
24. **Uziel T, Lerenthal Y, Moyal L, Andegeko Y, Mittelman L, Shiloh Y.** 2003. Requirement of the MRN complex for ATM activation by DNA damage. EMBO J **22:**5612–5621. http://dx.doi.org/10.1093/emboj/cdg541.
25. **Olson E, Nievera CJ, Lee AY, Chen L, Wu X.** 2007. The Mre11-Rad50-Nbs1 complex acts both upstream and downstream of ataxia telangiectasia mutated and Rad3-related protein (ATR) to regulate the S-phase checkpoint following UV treatment. J Biol Chem **282:**22939–22952. http://dx.doi.org/10.1074/jbc.M702162200.
26. **Carson CT, Schwartz RA, Stracker TH, Lilley CE, Lee DV, Weitzman MD.** 2003. The Mre11 complex is required for ATM activation and the G_2/M checkpoint. EMBO J **22:**6610–6620. http://dx.doi.org/10.1093/emboj/cdg630.
27. **Cervelli T, Palacios JA, Zentilin L, Mano M, Schwartz RA, Weitzman MD, Giacca M.** 2008. Processing of recombinant AAV genomes occurs in specific nuclear structures that overlap with foci of DNA-damage-

response proteins. J Cell Sci **121:**349–357. http://dx.doi.org/10.1242/jcs.003632.
28. **Lovric J, Mano M, Zentilin L, Eulalio A, Zacchigna S, Giacca M.** 2012. Terminal differentiation of cardiac and skeletal myocytes induces permissivity to AAV transduction by relieving inhibition imposed by DNA damage response proteins. Mol Ther **20:**2087–2097. http://dx.doi.org/10.1038/mt.2012.144.
29. **Lilley CE, Carson CT, Muotri AR, Gage FH, Weitzman MD.** 2005. DNA repair proteins affect the lifecycle of herpes simplex virus 1. Proc Natl Acad Sci U S A **102:**5844–5849. http://dx.doi.org/10.1073/pnas.0501916102.
30. **Shirata N, Kudoh A, Daikoku T, Tatsumi Y, Fujita M, Kiyono T, Sugaya Y, Isomura H, Ishizaki K, Tsurumi T.** 2005. Activation of ataxia telangiectasia-mutated DNA damage checkpoint signal transduction elicited by herpes simplex virus infection. J Biol Chem **280:**30336–30341. http://dx.doi.org/10.1074/jbc.M500976200.
31. **Wilkinson DE, Weller SK.** 2004. Recruitment of cellular recombination and repair proteins to sites of herpes simplex virus type 1 DNA replication is dependent on the composition of viral proteins within prereplicative sites and correlates with the induction of the DNA damage response. J Virol **78:**4783–4796. http://dx.doi.org/10.1128/JVI.78.9.4783-4796.2004.
32. **Stracker TH, Carson CT, Weitzman MD.** 2002. Adenovirus oncoproteins inactivate the Mre11-Rad50-NBS1 DNA repair complex. Nature **418:**348–352. http://dx.doi.org/10.1038/nature00863.
33. **Stracker TH, Lee DV, Carson CT, Araujo FD, Ornelles DA, Weitzman MD.** 2005. Serotype-specific reorganization of the Mre11 complex by adenoviral E4orf3 proteins. J Virol **79:**6664–6673. http://dx.doi.org/10.1128/JVI.79.11.6664-6673.2005.
34. **Evans JD, Hearing P.** 2005. Relocalization of the Mre11-Rad50-Nbs1 complex by the adenovirus E4 ORF3 protein is required for viral replication. J Virol **79:**6207–6215. http://dx.doi.org/10.1128/JVI.79.10.6207-6215.2005.
35. **Ferrari FK, Samulski T, Shenk T, Samulski RJ.** 1996. Second-strand synthesis is a rate-limiting step for efficient transduction by recombinant adeno-associated virus vectors. J Virol **70:**3227–3234.
36. **Fisher KJ, Gao GP, Weitzman MD, DeMatteo R, Burda JF, Wilson JM.** 1996. Transduction with recombinant adeno-associated virus for gene therapy is limited by leading-strand synthesis. J Virol **70:**520–532.
37. **Rabinowitz JE, Rolling F, Li C, Conrath H, Xiao W, Xiao X, Samulski RJ.** 2002. Cross-packaging of a single adeno-associated virus (AAV) type 2 vector genome into multiple AAV serotypes enables transduction with broad specificity. J Virol **76:**791–801. http://dx.doi.org/10.1128/JVI.76.2.791-801.2002.
38. **Xiao X, Li J, Samulski RJ.** 1998. Production of high-titer recombinant adeno-associated virus vectors in the absence of helper adenovirus. J Virol **72:**2224–2232.
39. **Haberman RP, McCown TJ, Samulski RJ.** 1998. Inducible long-term gene expression in brain with adeno-associated virus gene transfer. Gene Ther **5:**1604–1611. http://dx.doi.org/10.1038/sj.gt.3300782.
40. **Li C, Hirsch M, Carter P, Asokan A, Zhou X, Wu Z, Samulski RJ.** 2009. A small regulatory element from chromosome 19 enhances liver-specific gene expression. Gene Ther **16:**43–51. http://dx.doi.org/10.1038/gt.2008.134.
41. **Zolotukhin S, Potter M, Hauswirth WW, Guy J, Muzyczka N.** 1996. A "humanized" green fluorescent protein cDNA adapted for high-level expression in mammalian cells. J Virol **70:**4646–4654.
42. **Rubenwolf S, Schutt H, Nevels M, Wolf H, Dobner T.** 1997. Structural analysis of the adenovirus type 5 E1B 55-kilodalton-E4orf6 protein complex. J Virol **71:**1115–1123.
43. **Hewitt FC, Samulski RJ.** 2010. Creating a novel origin of replication through modulating DNA-protein interfaces. PLoS One **5:**e8850. http://dx.doi.org/10.1371/journal.pone.0008850.
44. **Xiao X, Li J, McCown TJ, Samulski RJ.** 1997. Gene transfer by adeno-associated virus vectors into the central nervous system. Exp Neurol **144:**113–124. http://dx.doi.org/10.1006/exnr.1996.6396.
45. **Farkas SL, Zadori Z, Benko M, Essbauer S, Harrach B, Tijssen P.** 2004. A parvovirus isolated from royal python (Python regius) is a member of the genus Dependovirus. J Gen Virol **85:**555–561. http://dx.doi.org/10.1099/vir.0.19616-0.
46. **Grieger JC, Choi VW, Samulski RJ.** 2006. Production and characterization of adeno-associated viral vectors. Nat Protoc **1:**1412–1428. http://dx.doi.org/10.1038/nprot.2006.207.
47. **Choi VW, McCarty DM, Samulski RJ.** 2006. Host cell DNA repair pathways in adeno-associated viral genome processing. J Virol **80:**10346–10356. http://dx.doi.org/10.1128/JVI.00841-06.
48. **Heffernan TP, Simpson DA, Frank AR, Heinloth AN, Paules RS, Cordeiro-Stone M, Kaufmann WK.** 2002. An ATR- and Chk1-dependent S checkpoint inhibits replicon initiation following UVC-induced DNA damage. Mol Cell Biol **22:**8552–8561. http://dx.doi.org/10.1128/MCB.22.24.8552-8561.2002.
49. **Nghiem P, Park PK, Kim Y, Vaziri C, Schreiber SL.** 2001. ATR inhibition selectively sensitizes G_1 checkpoint-deficient cells to lethal premature chromatin condensation. Proc Natl Acad Sci U S A **98:**9092–9097. http://dx.doi.org/10.1073/pnas.161281798.
50. **Theunissen JW, Kaplan MI, Hunt PA, Williams BR, Ferguson DO, Alt FW, Petrini JH.** 2003. Checkpoint failure and chromosomal instability without lymphomagenesis in Mre11(ATLD1/ATLD1) mice. Mol Cell **12:**1511–1523. http://dx.doi.org/10.1016/S1097-2765(03)00455-6.
51. **Yu Z, Vogel G, Coulombe Y, Dubeau D, Spehalski E, Hebert J, Ferguson DO, Masson JY, Richard S.** 2012. The MRE11 GAR motif regulates DNA double-strand break processing and ATR activation. Cell Res **22:**305–320. http://dx.doi.org/10.1038/cr.2011.128.
52. **Buis J, Wu Y, Deng Y, Leddon J, Westfield G, Eckersdorff M, Sekiguchi JM, Chang S, Ferguson DO.** 2008. Mre11 nuclease activity has essential roles in DNA repair and genomic stability distinct from ATM activation. Cell **135:**85–96. http://dx.doi.org/10.1016/j.cell.2008.08.015.
53. **Xiao PJ, Samulski RJ.** 2012. Cytoplasmic trafficking, endosomal escape, and perinuclear accumulation of adeno-associated virus type 2 particles are facilitated by microtubule network. J Virol **86:**10462–10473. http://dx.doi.org/10.1128/JVI.00935-12.
54. **Stewart GS, Maser RS, Stankovic T, Bressan DA, Kaplan MI, Jaspers NG, Raams A, Byrd PJ, Petrini JH, Taylor AM.** 1999. The DNA double-strand break repair gene hMRE11 is mutated in individuals with an ataxia-telangiectasia-like disorder. Cell **99:**577–587. http://dx.doi.org/10.1016/S0092-8674(00)81547-0.
55. **McCarty DM, Monahan PE, Samulski RJ.** 2001. Self-complementary recombinant adeno-associated virus (scAAV) vectors promote efficient transduction independently of DNA synthesis. Gene Ther **8:**1248–1254. http://dx.doi.org/10.1038/sj.gt.3301514.
56. **Asokan A, Schaffer DV, Samulski RJ.** 2012. The AAV vector toolkit: poised at the clinical crossroads. Mol Ther **20:**699–708. http://dx.doi.org/10.1038/mt.2011.287.
57. **D'Amours D, Jackson SP.** 2002. The Mre11 complex: at the crossroads of DNA repair and checkpoint signalling. Nat Rev Mol Cell Biol **3:**317–327. http://dx.doi.org/10.1038/nrm805.
58. **Cataldi MP, McCarty DM.** 2010. Differential effects of DNA double-strand break repair pathways on single-strand and self-complementary adeno-associated virus vector genomes. J Virol **84:**8673–8682. http://dx.doi.org/10.1128/JVI.00641-10.
59. **Sanlioglu S, Benson P, Engelhardt JF.** 2000. Loss of ATM function enhances recombinant adeno-associated virus transduction and integration through pathways similar to UV irradiation. Virology **268:**68–78. http://dx.doi.org/10.1006/viro.1999.0137.
60. **Allalunis-Turner MJ, Barron GM, Day RS, III, Dobler KD, Mirzayans R.** 1993. Isolation of two cell lines from a human malignant glioma specimen differing in sensitivity to radiation and chemotherapeutic drugs. Radiat Res **134:**349–354. http://dx.doi.org/10.2307/3578196.
61. **Ellis NA, Groden J, Ye TZ, Straughen J, Lennon DJ, Ciocci S, Proytcheva M, German J.** 1995. The Bloom's syndrome gene product is homologous to RecQ helicases. Cell **83:**655–666. http://dx.doi.org/10.1016/0092-8674(95)90105-1.
62. **Oshima J, Yu CE, Piussan C, Klein G, Jabkowski J, Balci S, Miki T, Nakura J, Ogihara T, Ells J, Smith M, Melaragno MI, Fraccaro M, Scappaticci S, Matthews J, Ouais S, Jarzebowicz A, Schellenberg GD, Martin GM.** 1996. Homozygous and compound heterozygous mutations at the Werner syndrome locus. Hum Mol Genet **5:**1909–1913. http://dx.doi.org/10.1093/hmg/5.12.1909.
63. **Tuo J, Jaruga P, Rodriguez H, Bohr VA, Dizdaroglu M.** 2003. Primary fibroblasts of Cockayne syndrome patients are defective in cellular repair of 8-hydroxyguanine and 8-hydroxyadenine resulting from oxidative stress. FASEB J **17:**668–674. http://dx.doi.org/10.1096/fj.02-0851com.
64. **Williams BR, Mirzoeva OK, Morgan WF, Lin J, Dunnick W, Petrini JH.** 2002. A murine model of Nijmegen breakage syndrome. Curr Biol **12:**648–653. http://dx.doi.org/10.1016/S0960-9822(02)00763-7.
65. **Bedford MT, Clarke SG.** 2009. Protein arginine methylation in mammals: who, what, and why. Mol Cell **33:**1–13. http://dx.doi.org/10.1016/j.molcel.2008.12.013.
66. **Hewitt FC, Li C, Gray SJ, Cockrell S, Washburn M, Samulski RJ.** 2009. Reducing the risk of adeno-associated virus (AAV) vector mobilization

with AAV type 5 vectors. J Virol **83:**3919–3929. http://dx.doi.org/10.1128/JVI.02466-08.
67. **Gautam D, Bridge E.** 2013. The kinase activity of ataxia-telangiectasia mutated interferes with adenovirus E4 mutant DNA replication. J Virol **87:**8687–8696. http://dx.doi.org/10.1128/JVI.00376-13.
68. **Trujillo KM, Sung P.** 2001. DNA structure-specific nuclease activities in the Saccharomyces cerevisiae Rad50*Mre11 complex. J Biol Chem **276:**35458–35464. http://dx.doi.org/10.1074/jbc.M105482200.
69. **de Jager M, Dronkert ML, Modesti M, Beerens CE, Kanaar R, van Gent DC.** 2001. DNA-binding and strand-annealing activities of human Mre11: implications for its roles in DNA double-strand break repair pathways. Nucleic Acids Res **29:**1317–1325. http://dx.doi.org/10.1093/nar/29.6.1317.
70. **Paull TT, Gellert M.** 1998. The 3′ to 5′ exonuclease activity of Mre 11 facilitates repair of DNA double-strand breaks. Mol Cell **1:**969–979. http://dx.doi.org/10.1016/S1097-2765(00)80097-0.
71. **Karen KA, Hearing P.** 2011. Adenovirus core protein VII protects the viral genome from a DNA damage response at early times after infection. J Virol **85:**4135–4142. http://dx.doi.org/10.1128/JVI.02540-10.
72. **Mathew SS, Bridge E.** 2007. The cellular Mre11 protein interferes with adenovirus E4 mutant DNA replication. Virology **365:**346–355. http://dx.doi.org/10.1016/j.virol.2007.03.049.
73. **Baker A, Rohleder KJ, Hanakahi LA, Ketner G.** 2007. Adenovirus E4 34k and E1b 55k oncoproteins target host DNA ligase IV for proteasomal degradation. J Virol **81:**7034–7040. http://dx.doi.org/10.1128/JVI.00029-07.
74. **Querido E, Blanchette P, Yan Q, Kamura T, Morrison M, Boivin D, Kaelin WG, Conaway RC, Conaway JW, Branton PE.** 2001. Degradation of p53 by adenovirus E4orf6 and E1B55K proteins occurs via a novel mechanism involving a Cullin-containing complex. Genes Dev **15:**3104–3117. http://dx.doi.org/10.1101/gad.926401.
75. **Schmidt M, Afione S, Kotin RM.** 2000. Adeno-associated virus type 2 Rep78 induces apoptosis through caspase activation independently of p53. J Virol **74:**9441–9450. http://dx.doi.org/10.1128/JVI.74.20.9441-9450.2000.
76. **Hirsch ML, Fagan BM, Dumitru R, Bower JJ, Yadav S, Porteus MH, Pevny LH, Samulski RJ.** 2011. Viral single-strand DNA induces p53-dependent apoptosis in human embryonic stem cells. PLoS One **6:**e27520. http://dx.doi.org/10.1371/journal.pone.0027520.
77. **Raj K, Ogston P, Beard P.** 2001. Virus-mediated killing of cells that lack p53 activity. Nature **412:**914–917. http://dx.doi.org/10.1038/35091082.
78. **Daya S, Cortez N, Berns KI.** 2009. Adeno-associated virus site-specific integration is mediated by proteins of the nonhomologous end-joining pathway. J Virol **83:**11655–11664. http://dx.doi.org/10.1128/JVI.01040-09.
79. **Babiss LE, Ginsberg HS, Darnell JE, Jr.** 1985. Adenovirus E1B proteins are required for accumulation of late viral mRNA and for effects on cellular mRNA translation and transport. Mol Cell Biol **5:**2552–2558.
80. **Halbert DN, Cutt JR, Shenk T.** 1985. Adenovirus early region 4 encodes functions required for efficient DNA replication, late gene expression, and host cell shutoff. J Virol **56:**250–257.
81. **Leppard KN, Shenk T.** 1989. The adenovirus E1B 55 kd protein influences mRNA transport via an intranuclear effect on RNA metabolism. EMBO J **8:**2329–2336.
82. **Samulski RJ, Shenk T.** 1988. Adenovirus E1B 55-Mr polypeptide facilitates timely cytoplasmic accumulation of adeno-associated virus mRNAs. J Virol **62:**206–210.
83. **Woo JL, Berk AJ.** 2007. Adenovirus ubiquitin-protein ligase stimulates viral late mRNA nuclear export. J Virol **81:**575–587. http://dx.doi.org/10.1128/JVI.01725-06.